doi:10.1038/nature11773

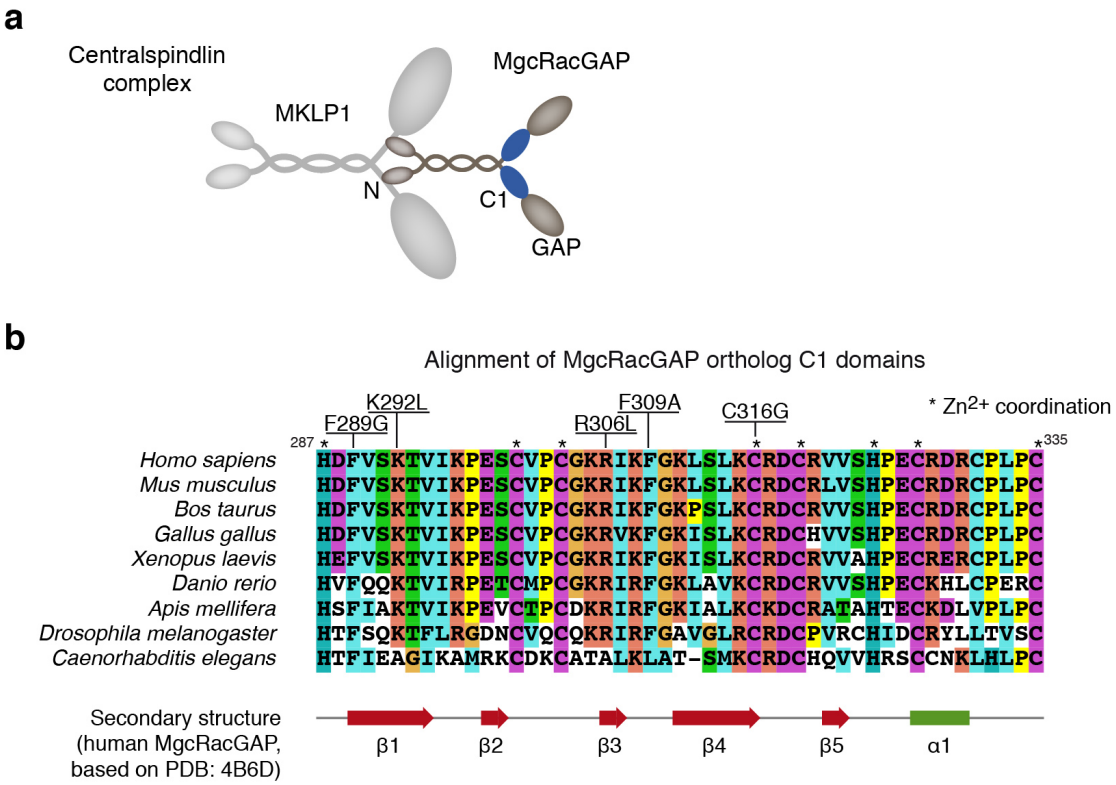

Figure S1 | Analysis of the C1 domain of MgcRacGAP.
a, Organization of the centralspindlin complex.
b, Sequence alignment of the C1 domains of MgcRacGAP orthologs. Sequences were aligned to amino acid positions 287 to 335 of human MgcRacGAP. Asterisks indicate conserved histidine and cysteine residues that are involved in zinc-coordination. Sequences (H. sapiens NP_037409, M. musculus NP_001240738, R. norvegicus NP_001101582, B. taurus XP_592496.2, G. gallus XP_424490, X. laevis NP_001084820, D. rerio NP_955925, A. mellifera XP_393627, D. melanogaster NP_610912 and C. elegans NP_499845) were aligned using ClustalX (www.clustal.org). The secondary structure of the C1 domain of human MgcRacGAP is illustrated below the alignment. The secondary structure was derived from PDB: 4B6D. α-helices and ß-sheets are illustrated by green rectangles and red arrows, respectively.

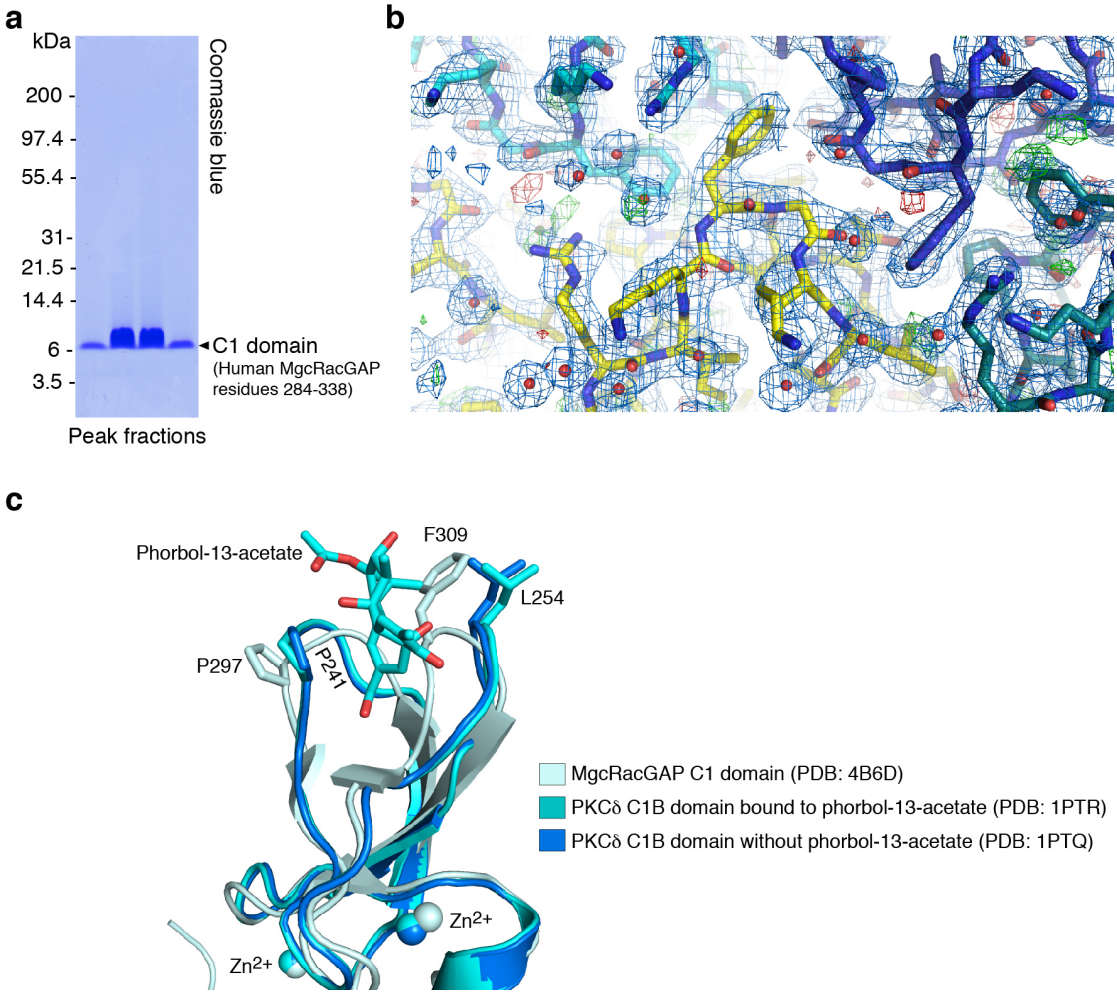

Figure S2 | Structure determination and analysis of the C1 domain of human MgcRacGAP using X-ray crystallography.

a, Ion exchange elution fractions of recombinant MgcRacGAP C1 domain were analyzed by Tricine-SDS-PAGE gel electrophoresis.

b, Example of the final weighted 2*Fo-Fc* (blue) and difference maps (negative - red, positive - green), contoured at 1 sigma; structure represented in stick format from four chains.

c, Superposition of MgcRacGAP's C1 domain (PDB: 4B6D, pale blue) with PKCδ in complex with phorbol-13-acetate (PDB: 1PTR, cyan)[1] and PKCδ without ligand (PDB: 1PTQ, blue)[1]. R.m.s.d. of Cα atoms between MgcRacGAP's C1 domain and PKCδ is 1.44 Å over 48 residues and between PKC delta structures is 0.27 Å over 50 residues using SSM[2]. The position of the F309-containing loop in MgcRacGAP's C1 domain structure results in narrower cleft that is likely to prevent phorbol ester binding due to steric hindrance.

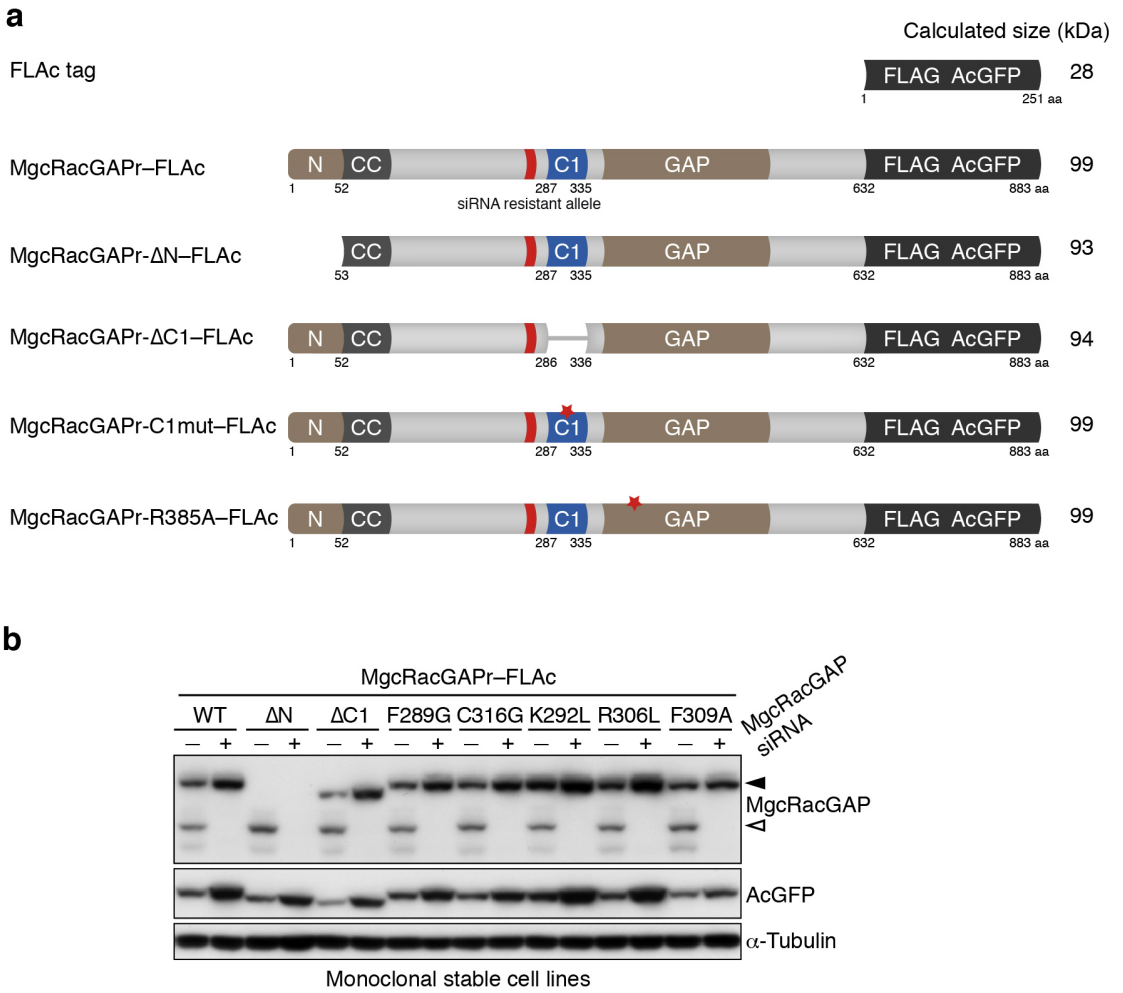

Figure S3 | Domain organization of MgcRacGAP transgenes and immunoblot characterization of monoclonal cell lines.
a, Domain organization of FLAc-tagged MgcRacGAP transgenes used to generate monoclonal cell lines.
b, Immunoblot analysis of lysates prepared from monoclonal HeLa Kyoto cell lines expressing the indicated MgcRacGAPr–FLAc variants after transfection with control (-) or MgcRacGAP siRNA (+). Extracts were prepared 48 h after transfection. Filled and open arrowheads indicate transgenic and endogenous proteins, respectively. Please note that the ΔN allele lacks the epitope recognized by the MgcRacGAP antibody.

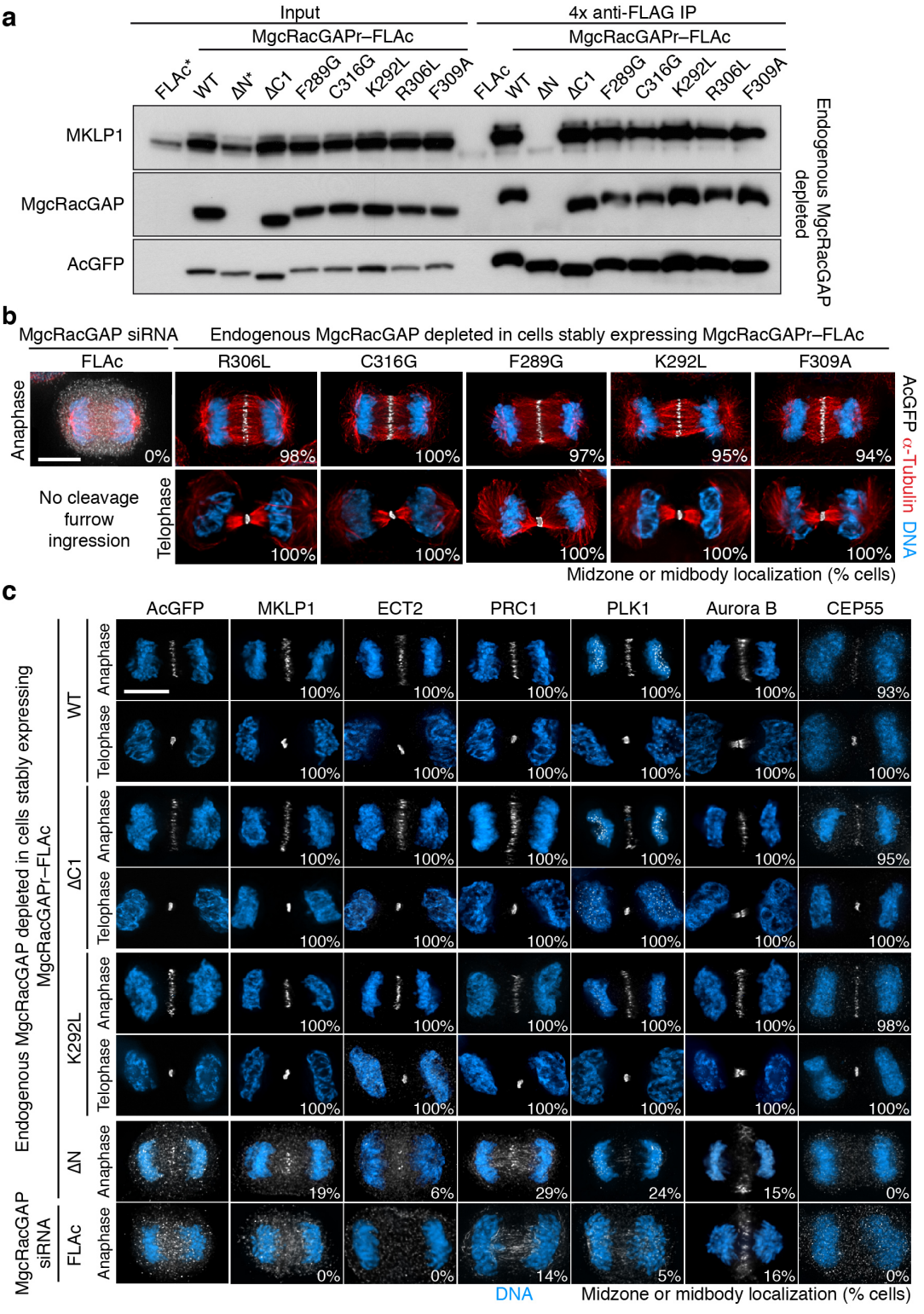

Figure S4 | The C1 domain of MgcRacGAP is dispensable for known properties and functions of the centralspindlin complex.

a, Immunoblot analysis of whole cell extracts (input) and immunoprecipitates (IP) prepared from monoclonal cell lines stably expressing the indicated transgenes. Extracts were prepared from nocodazole-arrested cells 48 h after transfection with MgcRacGAP siRNA. Extracts were subjected to immunoprecipitation using anti-

FLAG antibodies. * Please note that in the absence of MgcRacGAP-MKLP1 complex formation the abundance of both proteins is reduced in cell extracts (FLAc and ΔN).
b, IF analysis of monoclonal cell lines stably expressing the indicated transgenes (n>50 anaphase and telophase cells each).
c, IF analysis of AcGFP, MKLP1, ECT2, PRC1, PLK1, Aurora B and CEP55 in cells stably expressing the indicated transgenes (n>30 cells each). Scale bars, 10 μm.

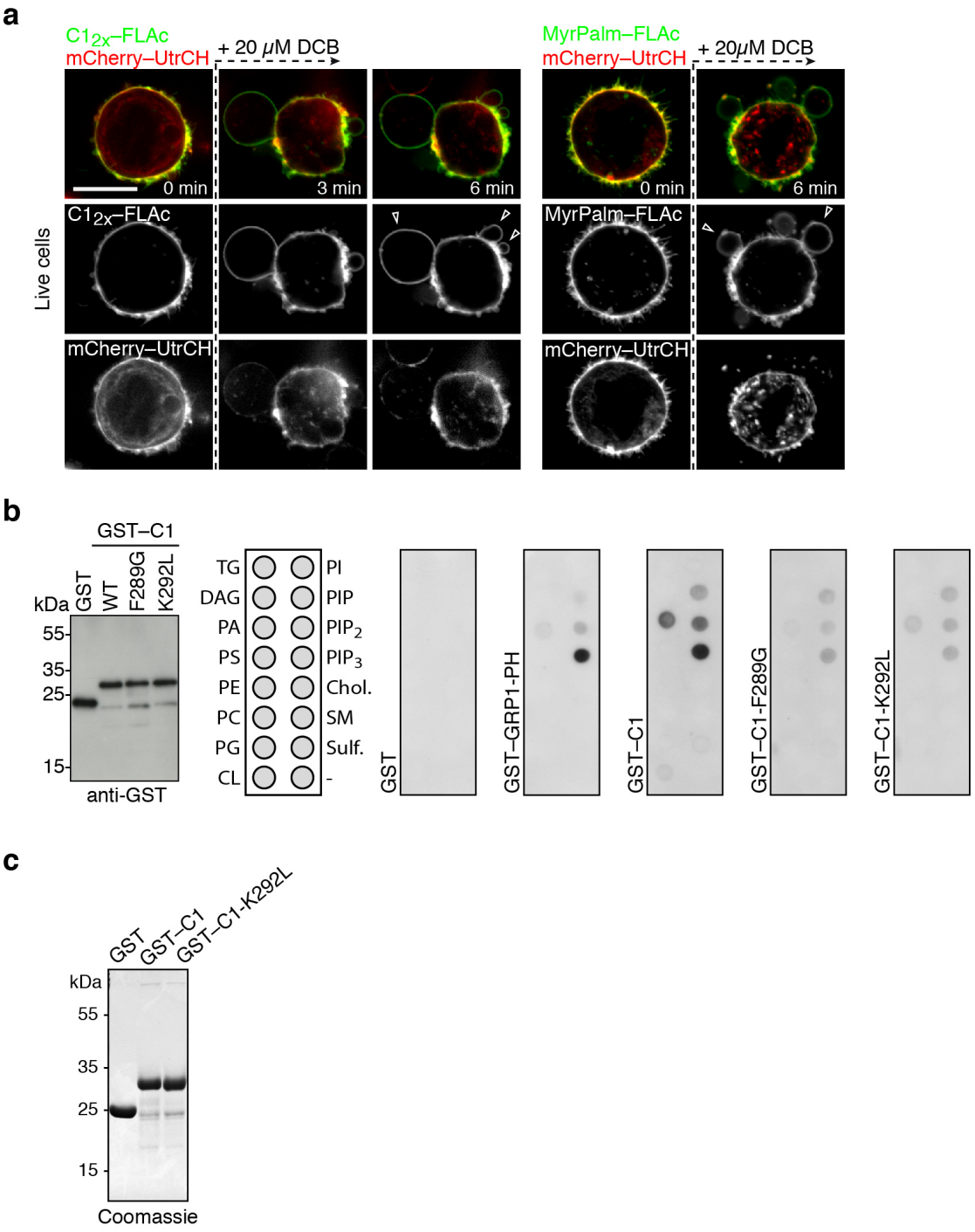

Figure S5 | Plasma membrane association and lipid interaction of MgcRacGAP's C1 domain.

a, Confocal live-cell imaging of mitotic cells co-expressing mCherry–UtrCH, a probe for filamentous actin[3], and C1$_{2x}$–FLAc or MyrPalm–FLAc. Cells were treated with 20 μM dihydrocytochalasin B (DCB), an actin poison, at the indicated time. Open arrowheads indicate membrane blebs. Scale bar, 10 μm. C1$_{2x}$–FLAc, like MyrPalm–FLAc, remained associated with the plasma membrane in blebs that were largely devoid of filamentous actin (7/7 cells). This suggests that the C1 domain of MgcRacGAP associates directly with the inner leaflet of the plasma membrane and not with the cortical actomyosin network.

b, Immunoblot analysis of recombinant purified glutathione-binding protein (GST) and GST–C1 fusion proteins (left panel). Lipid arrays were incubated with the indicated recombinant proteins and subsequently probed by anti-GST antibodies (right panel). Key: triglyceride (TG), diacylglycerol (DAG), phosphatidic acid (PA), phosphatidylserine (PS), phosphatidylethanolamine (PE); phosphatidylcholine (PC), phosphatidylglycerol (PG), cardiolipin (CL), phosphatidylinositol (PI), phosphatidylinositol 4-phosphate/ PI4P (PIP), phosphatidylinositol 4,5-bisphosphate/ PI(4,5)P_2 (PIP2), phosphatidylinositol 3,4,5, -trisphosphate/ PI(3,4,5)P_3 (PIP3), cholesterol (Chol.), sphingomyelin (SM), sulfatide (Sulf.).
c, Protein gel analysis of the recombinant proteins used for SPR analyses in Fig. 2e.

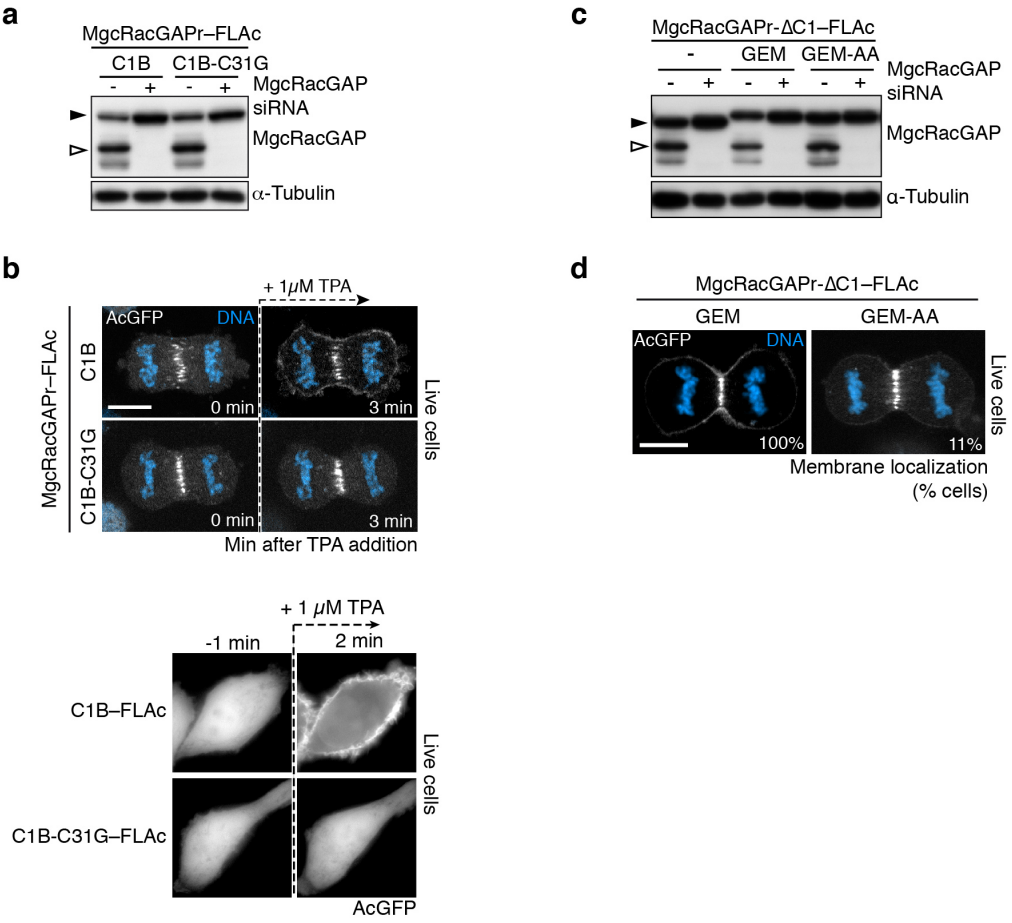

Figure S6 | Artificial tethering of MgcRacGAP to the plasma membrane.
a, Immunoblot analysis of protein extracts prepared from monoclonal cell lines expressing MgcRacGAPr–C1B–FLAc or MgcRacGAPr–C1B–C316G-FLAc. Extracts were prepared 48 h after transfection with control siRNA (-) or MgcRacGAP siRNA (+) duplexes. Filled and open arrowheads indicate transgenic and endogenous MgcRacGAP protein, respectively.
b, Confocal live-cell imaging of cells expressing MgcRacGAPr-C1B–FLAc or MgcRacGAPr-C1B-C316G–FLAc (top panel). Cells were treated with 1 µM TPA at the indicated time. Scale bar in this panel and the following panels represents 10 µm. Live-cell imaging of cells expressing a FLAc-tagged version of wild-type or C31G mutant C1B domain derived from human PKCα (bottom panel). Cells were treated with 1 µM TPA at t=0 min.
c, Immunoblot analysis of protein extracts prepared from monoclonal cell lines expressing the indicated transgenes. Extracts were prepared 48 h after transfection with control siRNA (-) or MgcRacGAP siRNA (+) duplexes.
d, Confocal live-cell imaging of cells expressing the indicated transgenes (n > 50 cells each). Scale bars, 10 µm.

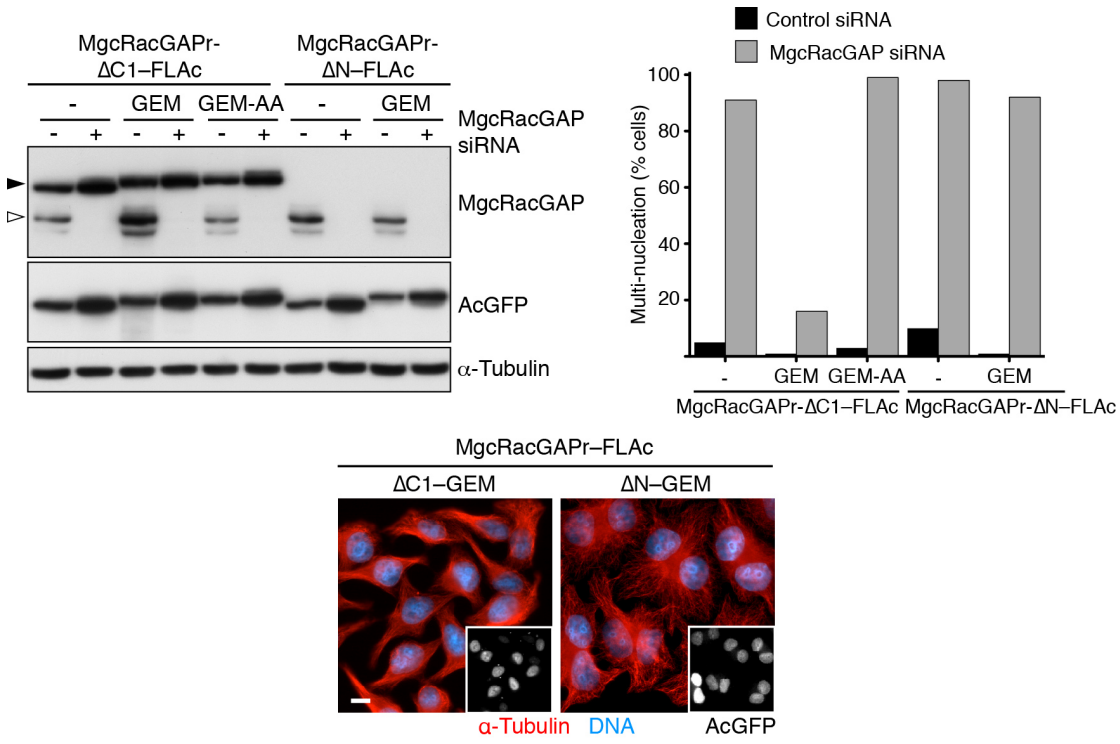

Figure S7 | Insertion of the polybasic tail of GEM into MgcRacGAP-ΔN does not restore cytokinesis.
Immunoblot analysis of protein extracts prepared from stable HeLa Kyoto cell lines expressing the indicated transgenes (left panel). Extracts were prepared 48 h after transfection with control siRNA (-) or MgcRacGAP siRNA (+) duplexes. Quantification of the percentage of multi-nucleated interphase cells (multi-nucleation) (n > 200 cells) (right panel). IF microscopy analysis of the indicated cell lines 48 h after transfection with MgcRacGAP siRNA (bottom panel). Scale bar, 10 μm.

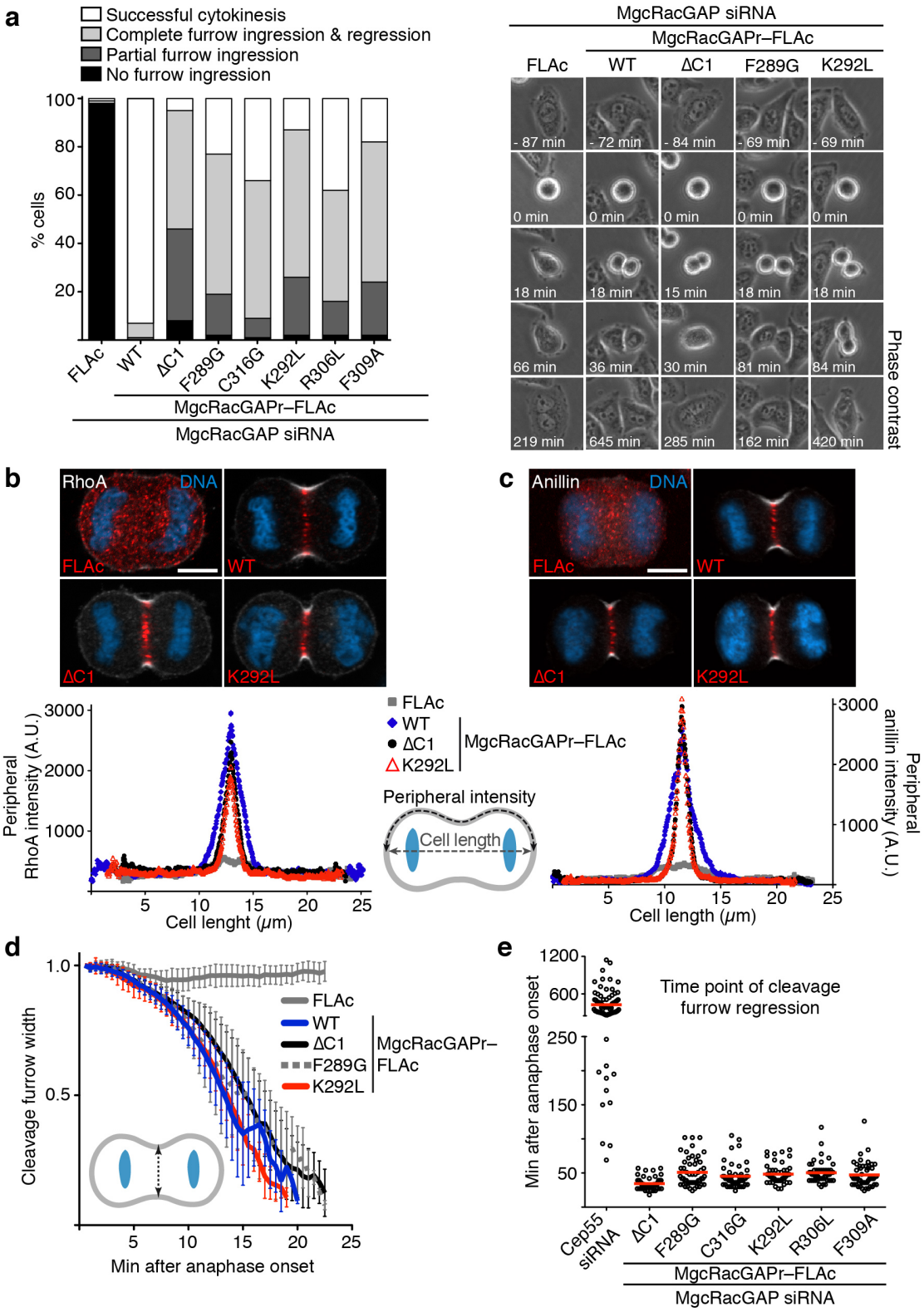

Figure S8 | Analysis of cytokinetic dynamics.
a, Quantification of cytokinesis phenotypes in monoclonal cell lines expressing the indicated transgenes. Mono-nucleated cells entering mitosis were analyzed from 30 to 48 h after transfection with MgcRacGAP siRNA (n>103 cells each) (left panel). Representative cell division phenotypes of selected cell lines are shown as a time-

lapse series (right panel). Time point t = 0 min was set to the metaphase-to-anaphase transition.
b, IF analysis of RhoA in anaphase cells expressing the indicated transgenes (images, top panel). Cells were fixed 48 h after transfection with MgcRacGAP siRNA. Quantification of the peripheral RhoA intensity in monoclonal cell lines expressing the indicated transgenes (n>10 cells each) (graph, bottom panel). In the graph, the mean intensity of RhoA staining along the periphery of anaphase cells was plotted against cell length. Scale bar, 10 μm.
c, IF analysis of anillin in anaphase cells (n>10 cells). The analysis and quantification was performed as described for RhoA in (B).
d, Quantification of the cleavage furrow ingression rate in cells expressing the indicated transgenes. Cells were analyzed 30 h after transfection with MgcRacGAP siRNA. High-resolution differential interference contrast microscopy images were acquired in 30 sec intervals. The cleavage furrow width was normalized to the cell diameter at metaphase for each cell analyzed. Time point t = 0 min was set to the metaphase-to-anaphase transition. Error bars represent standard deviation (n=10 cells for each transgene).
e, Analysis of the time point of cleavage furrow regression. Graph displays the time from the metaphase-to-anaphase transition (t = 0 min) to the beginning of cleavage furrow regression in non-transgenic cells (CEP55 siRNA) or cells that express the indicated MgcRacGAP transgenes (n>50 cells). Red line in scatter blot marks the mean. Mono-nucleated cells that enter mitosis and display full furrow ingression were analyzed between 30 and 48 h after transfection with CEP55 or MgcRacGAP siRNA.

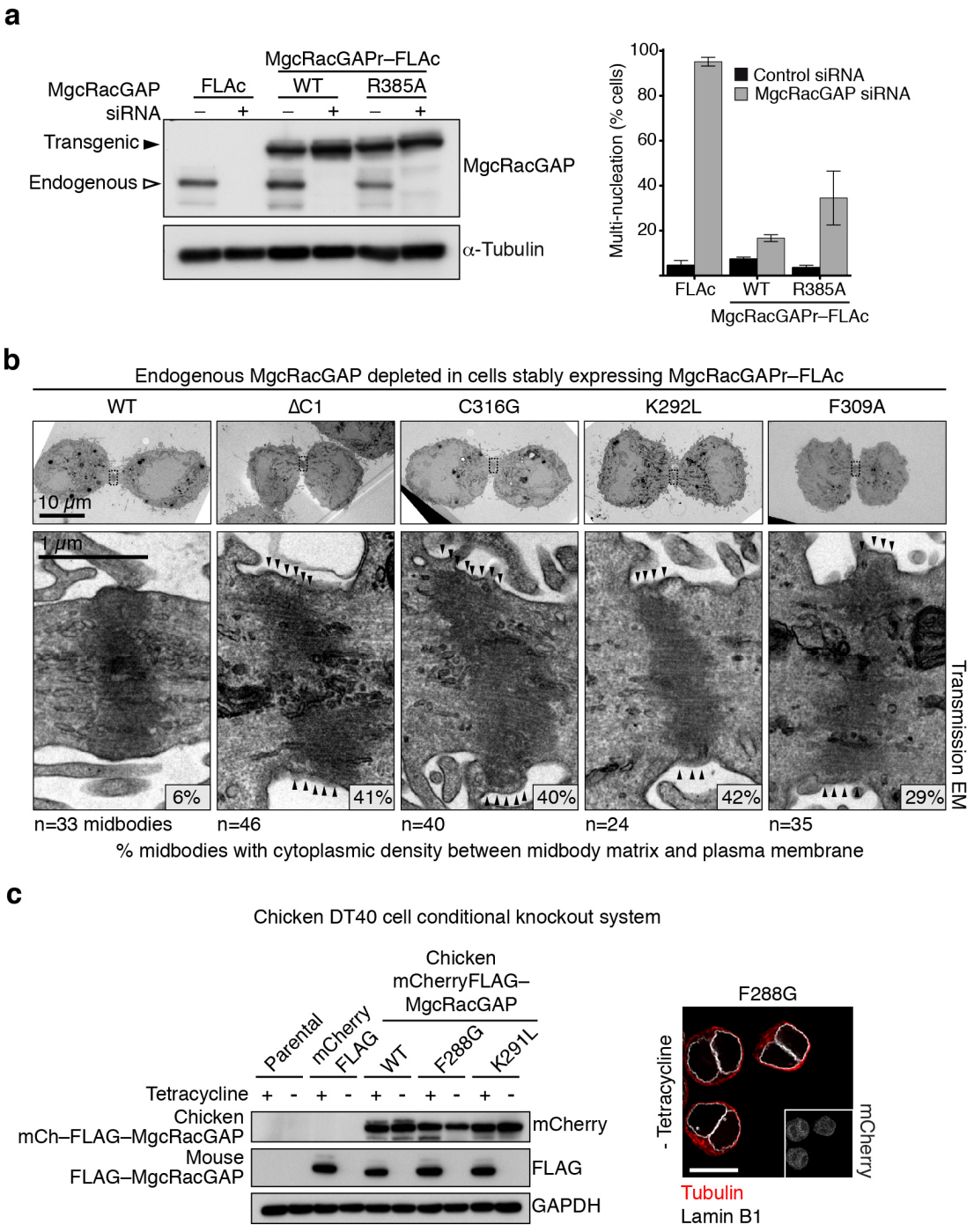

Figure S9 | Analysis of MgcRacGAP function in human and chicken cells.
a, Immunoblot analysis of protein extracts prepared from monoclonal HeLa Kyoto cell lines expressing the indicated transgenes (left panel). Extracts were prepared 48 h after transfection with control siRNA (-) or MgcRacGAP siRNA (+) duplexes. Multi-nucleation of AcGFP-positive interphase cells in monoclonal lines expressing the indicated transgenes (n>200 cells each) (graph, right panel). Error bars represent standard deviation of three experiments.
b, Transmission EM of cells stably expressing the indicated transgenes. Cells were transfected with MgcRacGAP siRNA, fixed 100 min after release from metaphase. Arrowheads indicate gaps between the midbody matrix and the plasma membrane. (n>23 midbodies; exact sample sizes are specified below the corresponding images).

c, Immunoblot analysis of extracts prepared from parental wild-type DT40 cells or modified MgcRacGAP conditional knockout DT40 cells (left panel). Expression of mouse FLAG–MgcRacGAP is tetracycline-inducible. Extracts were prepared after cells were cultured for 48 h in the presence or absence of tetracycline. IF analysis of MgcRacGAP conditional knockout DT40 cell lines stably expressing chicken mCherry–FLAG–MgcRacGAP-F288G transgenes 48 h after withdrawal of tetracycline. Scale bar, 10 μm.

References for Supplementary Figures

1 Zhang, G., Kazanietz, M. G., Blumberg, P. M. & Hurley, J. H. Crystal structure of the cys2 activator-binding domain of protein kinase C delta in complex with phorbol ester. *Cell* **81**, 917-924, (1995).

2 Krissinel, E. & Henrick, K. Secondary-structure matching (SSM), a new tool for fast protein structure alignment in three dimensions. *Acta Crystallogr. D. Biol. Crystallogr.* **60**, 2256-2268, (2004).

3 Burkel, B. M., von Dassow, G. & Bement, W. M. Versatile fluorescent probes for actin filaments based on the actin-binding domain of utrophin. *Cell Motil. Cytoskelet.* **64**, 822-832, (2007).

Supplementary Table 1. Data collection, phasing and refinement statistics.

Data Collection	Zn SAD	
Wavelength (Å)	1.283	0.9795
Space Group	$P2_1$	$P2_1$
Unit cell parameters:		
a, b, c (Å)	36.9, 134.2, 56.8	36.9, 133.9, 56.7
α, β, γ (°)	90.0, 108.9, 90.0	90.0, 109.0, 90.0
No. crystals used	4	1
Resolution (Å)	53.7-2.53 (2.60-2.53) [a]	66.9-2.20 (2.32-2.20)
No. of Reflections:		
Measured	273,551 (16,805)	253,030 (33,555)
Unique	17,384 (1,312)	26,140 (3,775)
Completeness (%)	99.3 (99.5)	99.4 (98.8)
Anomalous Completeness (%)	99.2 (99.5)	
Multiplicity	15.7 (12.8)	9.7 (8.9)
Anomalous Multiplicity	7.6 (6.1)	
$\langle I/\sigma(I)\rangle$	10.8 (3.4)	9.4 (2.6)
R_{merge}	0.21 (1.2)	0.15 (0.96)
R_{pim} (all I^+ and I^-)	0.058 (0.36)	0.052 (0.34)
DelAnom $CC_{1/2}$ [b]:		
53.7-11.31 Å	0.409	
2.60-2.53 Å	0.076	
Overall	0.577	
SAD Phasing Statistics		
No. of Zn sites refined	12	
FoM to 2.8 Å [c]	0.38	
FoM (DM) to 2.53 Å [d]	0.80	
Refinement Statistics		
Resolution Range ($Å^2$)		66.9-2.20
No. of Reflections:		
Work Set		24,803
Free		1,308
R_{work}/R_{free}		0.210/0.235
No. of Atoms:		
Total		2,932
Protein		2,751
Zn		12
Solvent		163
R.m.s. Deviations from Ideal Values		
Bonds (Å)		0.007
Angles (°)		1.128
Average B factor ($Å^2$)		56.8
Ramachandran Plot Quality [e]:		
Most Favored (%)		98.0
Disallowed (%)		0

[a] Values in parentheses correspond to the highest resolution bin.
[b] DelAnom correlation between half sets for the lowest and highest resolution shells and for the whole dataset.
[c] Figure of merit for acentric reflections, computed to 2.8 A.
[d] Overall figure of merit after density modification in Solomon assuming solvent content of 68%.
[e] Analyzed using Molprobity (http://molprobity.biochem.duke.edu/).